Hindawi
Modelling and Simulation in Engineering
Volume 2018, Article ID 7329014, 12 pages
https://doi.org/10.1155/2018/7329014

Research Article

Numerical Analysis of a Real Photovoltaic Module with Various Parameters

Costica Nituca,[1] Gabriel Chiriac,[1] Dumitru Cuciureanu,[2] Guoqiang Zhang,[3] Dong Han,[3] and Adrian Plesca[1]

[1]*Faculty of Electrical Engineering, "Gheorghe Asachi" Technical University of Iasi, Profesor Dimitrie Mangeron, No. 23, 700050 Iasi, Romania*
[2]*Q SRL, Stradela Sfantul Andrei, No. 13, Iasi, Romania*
[3]*Institute of Electrical Engineering, Chinese Academy of Sciences, No. 6, Beiertiao, Zhongguancun, Beijing, China*

Correspondence should be addressed to Gabriel Chiriac; gchiriac@tuiasi.ro

Received 19 December 2017; Accepted 29 January 2018; Published 20 March 2018

Academic Editor: Ricardo Perera

This article presents a real photovoltaic module with modeling and simulations starting from the model of a photovoltaic (PV) cell. *I-V*, *P-V*, and *P-I* characteristics are simulated for different solar irradiation, temperatures, series resistances, and parallel resistances. For a real photovoltaic module (ALTIUS Module AFP-235W) there are estimated series and parallel resistances for which the energetical performances of the module have optimal values for a solar radiation of 1000 W/m^2 and a temperature of the environment of 25°C. Temperature influence over the PV module performances is analyzed by using a thermal model of the ALTIUS Module AFP-235W using the finite element method. A temperature variation on the surface of the PV module is starting from a low value 40.15°C to a high value of 52.07°C. Current and power estimation are within the errors from 1.55% to about 4.3%. Experimental data are measured for the photovoltaic ALTIUS Module AFP-235W for an entire daylight.

1. Introduction

Solar energy is a renewable and no pollution energy with a significant annual riseup and this trend follows an ascending path. Locally produced renewable energy is more and more promoted as a key to the affordable and sustainable energy in remote area, in small communities, or for small consumers even into the large cities. Photovoltaic systems are realized form photovoltaic (PV) cells; one of the major advantages of photovoltaic cells is that they are highly modular and by proper scaling, they can be expected to provide adequate power for various loads [1]. These cells depend on photovoltaic effect for converting solar radiation into electricity and the generated photocurrent is proportional to the solar irradiation [2]. The output characteristics of a PV cell are nonlinear and fluctuate with solar radiation, cell temperature, series and parallel resistance, and other parameters of the mathematical model [3].

The modeling and simulation of the photovoltaic modules began long ago, but improvements of these models are analyzed and presented continually [2, 4–6]. The implementation of mathematical model of photovoltaic cell into specialized software MATLAB-Simulink is widely used. The computing models are realized by using the equations for the parameters as thermal voltage, photovoltaic current, diode saturation current, and ideality factor. The main characteristics can be obtained, such as the current-voltage (*I-V*) and power-voltage (*P-V*) characteristics [1, 4, 7–10]. The series and parallel resistances have an important influence over the PV cell parameters and these resistances are considered into the mathematical models, but in some cases [11–13] the series resistance is neglected into the model and in some cases [13–17] the parallel resistance is neglected. Thermal analysis of the photovoltaic panels is an important part of the studies in order to estimate the temperature distribution in a PV module and to determine the operating temperature of solar system accurately. Optical parameters for the reflectivity, transmissivity, and absorptivity for the relevant layers of the module are taken into account to determine the heat dissipation in the areas exposed directly to sunlight. Heat losses by convection and radiation are also included in simulations [18]. Finite element analysis is considered by

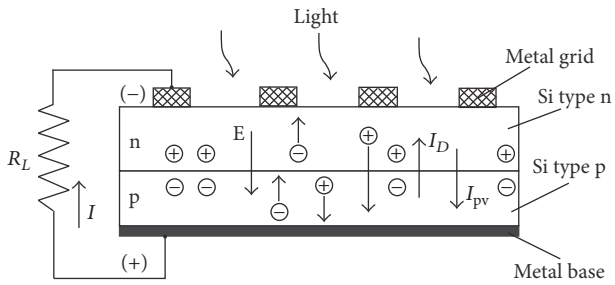

Figure 1: Physical structure of the photovoltaic cell.

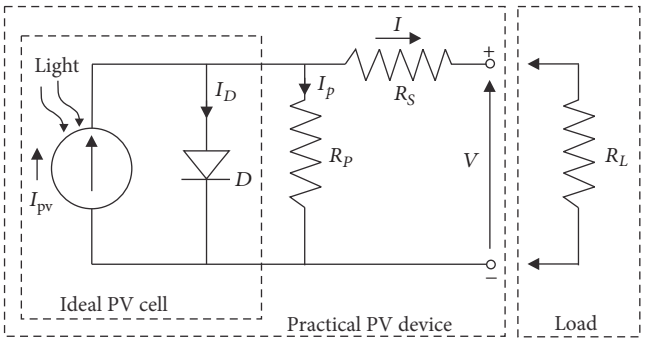

Figure 2: Equivalent model of a PV cell.

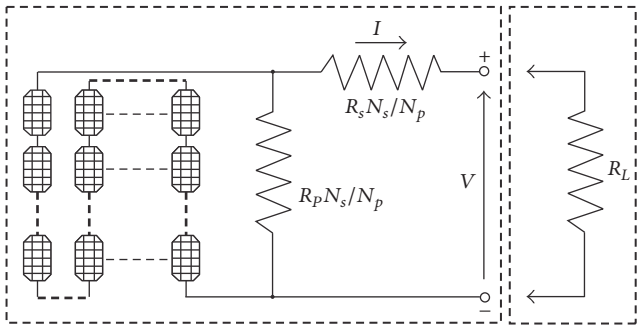

Figure 3: The PV module equivalent circuit model.

many researchers [18–21]. Also empirical models are used for the photovoltaic devices [22].

Different studies consider cooling system in order to reduce the operating temperature of the PV panel and to increase the performance of it [19, 23, 24].

In this article a model of the photovoltaic module is developed and the influence of some parameters are analyzed as series and parallel resistances, temperature, and solar irradiation over the PV module output characteristics. Simulations of module characteristics are realized considering the real data of a PV module ALTIUS AFP 235 and a thermal analysis and thermal simulation is also realized. There are also some experimental data analyzed and registered for an ALTIUS 235 module which is in regular use. The authors outline the variation of main electrical characteristics of a real PV module depending on solar radiation and also the correlation of the suitable functionality of the PV module with the temperature.

2. Modeling the Photovoltaic Module

2.1. Ideal PV Cell. The photovoltaic (PV) cell is considered as a semiconductor diode which is exposed to the solar radiation (Figure 1). A part of this radiation is absorbed by the *pn* junction creating pairs of electron hole. These electrical charges are separated by the electric field E: the electrons migrate in the "*n*" area and the holes migrate in the "*p*" area. This separation is the photovoltaic effect and it generates an electric current. This situation can be modeled into a simplified model having a current source in parallel with an ideal diode, with a photovoltaic current I_{pv} and a diode current I_D. Practical aspects of the PV cell can be studied considering a single-diode PV model with a series resistance R_s and a parallel resistance R_p (Figure 2).

The main equations to describe the *I-V* characteristics of an ideal PV cell are [1, 4, 7]

$$I = I_{pv} - I_D, \tag{1}$$

$$I_D = I_0 \left[\exp\left(\frac{qV}{akT} - 1\right)\right], \tag{2}$$

$$I = I_{pv} - I_0 \left[\exp\left(\frac{qV}{akT}\right) - 1\right]. \tag{3}$$

2.2. Modeling the PV Module. Many researches [1, 5, 9, 10] show that, for the analysis of the PV cells, there are some necessary supplementary parameters to be used into (3):

$$I = I_{pv} - I_0 \left[\exp\left(\frac{V + R_s I}{aV_T}\right) - 1\right] - \frac{V + R_s I}{R_p}, \tag{4}$$

where

$$V_T = \frac{kT}{q}. \tag{5}$$

In order to assure the parameters required on the consumers, a photovoltaic system has to be made by a sufficient number of PV cells, connected in series or in parallel, usually called modules or arrays. Figure 3 presents the equivalent circuit model of a photovoltaic system.

For the structure module in Figure 3, (4) will be [5, 8]

$$I = I_{pv}N_p - I_0N_p \left[\exp\left(\frac{V + IR_s\left(N_s/N_p\right)}{aV_TN_s}\right) - 1\right] - \frac{V + IR_s\left(N_s/N_p\right)}{R_p\left(N_s/N_p\right)}. \tag{6}$$

Based on the same characteristic, the following items are to be considered as well: the open circuit voltage/temperature coefficient (K_V), the short circuit current/temperature coefficient (K_I), and the maximum experimental peak output power ($P_{max,e}$) [5]. These aspects are related to the nominal condition

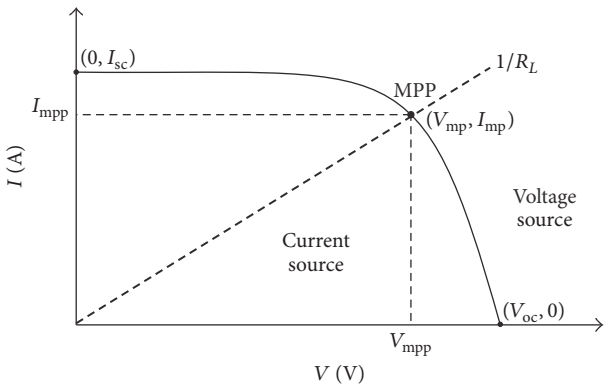

FIGURE 4: I-V characteristic of a practical photovoltaic device.

or to the Standard Test Conditions (STC). In these conditions the photovoltaic device has series resistances R_s with a strong impact when the system operates in the voltage source area and a parallel resistance R_p with a strong influence when the system operates in the current source area. In some cases [11–13] the R_s resistance is neglected into the model and in some cases [13–17] the R_p resistance is neglected.

For some points on the characteristic in Figure 4 (the short circuit $(0, I_{sc})$, open circuit $(V_{0c}, 0)$, and Maximum Power Point (V_{mpp}, I_{mpp})), the relations it can be written as follows[9]:

$$0 = I_{pv,n} - I_{0,n}\left[\exp\left(\frac{V_{0c,n}}{V_{T,n}}\right) - 1\right],$$
$$I_{mpp,n} = I_{pv,n} - I_{0,n}\left[\exp\left(\frac{V_{mpp,n} + R_s I_{mpp,n}}{V_{T,n}}\right) - 1\right]. \quad (7)$$

The current generated by the photovoltaic panel depends directly on the solar irradiation and is influenced by the temperature according to the next relation [26, 27]:

$$I_{pv} = \left(I_{pv,n} + K_I \Delta T\right)\frac{G}{G_n}, \quad (8)$$

where

$$\Delta T = T - T_n. \quad (9)$$

The nominal open voltage can be influenced by the temperature according to the relation [14]:

$$V_{0c} = V_{0c,n}\left(1 + K_V \Delta T\right) + V_T \ln\left(\frac{G}{G_n}\right). \quad (10)$$

The saturation current of the diode depends also on the temperature [5, 28, 29]:

$$I_0 = I_{0,n}\left(\frac{T_n}{T}\right)^3 \exp\left[\frac{qE_g}{ak}\left(\frac{1}{T_n} - \frac{1}{T}\right)\right], \quad (11)$$

where E_g is the band gap energy of the semiconductor (E_g = 1.12 eV for the polycrystalline Si at 25°C). The value of the saturated nominal current is given by [5]

$$I_{0,n} = \frac{I_{sc,n}}{\exp\left(V_{0c,n}/aV_{T,n}\right) - 1}. \quad (12)$$

Some researches [5, 30, 31] suggest an improving of the saturation current on the diode established by (10). The current $I_{pv,n}$ can be assumed to be approximately equal to I_{sc}, which is a very common assumption in PV modeling [5]. The assumption gives a good approximation because the series resistance is usually very small and the parallel resistance is large [5, 10]. In these conditions the saturation current on diode becomes

$$I_0 = \frac{I_{sc,n} + K_I \Delta T}{\exp\left(\left(V_{0c,n} + K_V \Delta T\right)/aN_c V_t\right) - 1}. \quad (13)$$

The performances of a PV cell depend also on the fill factor (FF), which is the ratio between the Maximum Power of a cell and the power of an ideal PV cell in the same operating conditions.

For a variable resistive load R_L connected at the cell output the power will be at maximum when the resistance R_L will have an optimal value R_{Lopt} equal to the ratio between the voltage V_{mpp} and the current I_{mpp}, Figure 4. Thus, the theoretical Maximum Power generated by the PV cell will be equal to the product between the V_{oc} and I_{sc}.

In these conditions, the fill factor (FF) is defined by

$$FF = \frac{P_{max,e}}{I_{sc}V_{oc}} = \frac{I_{mpp}V_{mpp}}{I_{sc}V_{oc}}. \quad (14)$$

The efficiency is calculated as the ratio between the power in MPP (for a specific temperature) and the power of the solar irradiation:

$$\eta = \frac{P_{mpp}}{A_{cell}G}. \quad (15)$$

3. The Effect of the Series and Parallel Resistances on the PV Cell Performances

The series and parallel resistances (R_s and R_p) have an important influence on the fill factor FF decreasing. Its value will decrease with R_s increasing and R_p decreasing. It is noteworthy that the series resistance R_s depends mainly on the internal resistances of the semiconductor devices, on the contact resistances, and on the electrical wires resistances and it has to be as low as possible. In the same time, the parallel resistance R_p depends on the metallic bridges between the edges of the junction, on the material defects (where losses' currents can appear, which can short-circuit the *pn* junction). Usually, its value is high, from thousands to tenth of thousands of ohms.

The relation between R_s and R_p can be estimated starting from the equality $P_{max,m} = P_{max,e}$, resulting in the relation for the resistance R_p [5, 10]:

$$P_{\mathrm{mac},m} = V_{\mathrm{mpp}} \left\{ I_{\mathrm{pv}} - I_0 \left[\exp\left(\frac{q}{kT} \frac{V_{\mathrm{mpp}} + R_s I_{\mathrm{mpp}}}{aN_s} \right) - 1 \right] - \frac{V_{\mathrm{mpp}} + R_s I_{\mathrm{mpp}}}{R_p} \right\} = P_{\mathrm{max},e},$$
$$R_p = \frac{V_{\mathrm{mpp}} + I_{\mathrm{mpp}} R_s}{\left\{ I_{\mathrm{pv}} V_{\mathrm{mpp}} - I_0 V_{\mathrm{mpp}} \exp\left[(q/kT) \left(\left(V_{\mathrm{mpp}} + I_{\mathrm{mpp}} R_s \right) / aN_s \right) \right] + I_0 V_{\mathrm{mpp}} - P_{\mathrm{max},e} \right\}}. \quad (16)$$

This equation is solved by successive iterations until it results in the best solution for the PV device. The solution has to concede with the maximum of the points V_{mpp} and I_{mpp}, on the I-V characteristic (Figure 4). In these conditions, the following with be the results [10]:

$$\mathrm{I}_{\mathrm{pv},n} = \frac{R_p + R_s}{R_p} I_{\mathrm{sc},n}. \quad (17)$$

The initial value for R_s is considered as zero, while the value for R_p is given by [7]

$$R_{p,\min} = \frac{V_{\mathrm{mpp}}}{I_{\mathrm{sc},n} - I_{\mathrm{mpp}}} - \frac{V_{0c,n} - V_{\mathrm{mpp}}}{I_{\mathrm{mpp}}}. \quad (18)$$

4. Numerical Modeling and Simulations of a Real Photovoltaic Module

Using the parameters of the ALTIUS AFP 235 Module (Table 1) and the adjusted parameters at nominal operating conditions (Table 2) simulations were realized in MATLAB-Simulink.

The results of the simulations are presented as I-V, P-V, and P-I characteristics in Figures 5–16 for different solar irradiation, temperatures, series resistances, and parallel resistances.

Figures 5, 6, and 7 present the I-V, P-V, and P-I characteristics for a constant temperature (25°C) and for different solar radiations (from 200 W/m^2 to 1000 W/m^2). From Figure 5, with the increase of the solar radiation the current will increase as a result and from Figure 6 the voltage will increase, which will increase the generated power. Figures 8, 9, and 10 present the I-V, P-V, and P-I characteristics for a constant radiation (1000 W/m^2) and for different temperatures of the environment (from −20°C to 60°C). It is to observed that, with the increasing of the temperature, the current will have a low increase while the voltage will decrease significantly. In this case the power delivered by the PV module will decrease significantly.

Figures 11, 12, and 13 present the I-V, P-V, and P-I characteristics for a constant value of the parallel resistance $R_p = 260\,\Omega$, for different values for the series resistance R_s ($R_s = 0.3\,\Omega$, $R_s = 0.9\,\Omega$, and $R_s = 1.5\,\Omega$), and for standard testing conditions STC (1000 W/m^2 and 25°C). It is to observed that, for a high value of the resistances R_s, the results will be a decrease in the current and the voltage and, accordingly, a decrease in the generated power. This influence is better to observe near the Maximum Power Point, where both the Maximum Power and the fill factor FF have low values. In this situation it is necessary to have a series resistance as low as possible, very close to zero value.

Figures 14, 15, and 16 present the I-V, P-V, and P-I characteristics for a constant series resistance $R_s = 0.3\,\Omega$, for different values for the parallel resistance R_p ($R_p = 260\,\Omega$, $R_p = 54\,\Omega$, and $R_p = 20\,\Omega$), and for standard testing conditions STC (1000 W/m^2 and 25°C). It is to observed that, for a low value of the parallel resistance, the results will be decreasing the value for the fill factor and power. For a better operation of the PV cell, it is necessary to have a parallel resistance as high as possible.

From all the above characteristics we can say that the energetical performances of the ALTIUS Module AFP-235W have optimal values when the series resistance is $R_s = 0.3\,\Omega$ and the parallel resistance is $R_p = 260\,\Omega$, for a solar radiation of 1000 W/m^2 and a temperature of the environment of 25°C.

5. Temperature Influence over the PV Module Performances

The increase in the environment temperature and in the thermal radiation has a negative influence over the energetical performances of the PV system. To study these aspects, a thermal model of the ALTIUS Module AFP-235W using the finite element method was realized. The properties of the materials used on the module are presented in Table 3.

The photovoltaic panel is a capsuled system realized from many successive layers. Thus, it is necessary to have a high thermal conductivity in order to assure good cooling of the PV cells. Considering this construction in layers, the thermal transfer is realized between the layers by conduction, convection, and radiation. Thermal analysis by the finite element method supposes an establishment of the thermal equilibrium for every volume zone dV.

$$P_c = P_t - P_r + P_a. \quad (19)$$

The left term of the equation is the heating power from the current flow, P_c. It is in balance with the heat stored by temporal change of temperature P_t, the power removed from the element by thermal conduction P_r, and the thermal power dissipated to the surrounding area by the surface convection, P_a. For P_c, P_t, P_r, and P_a, the following equations can be written:

Table 1: Parameters of the Altius, AFP 235 solar module at 25°C, 1000 W/m^2 [25].

Name-specifications from data sheet	AFP 235
Maximum Power (Pmax,e)	239.99 Wp
Voltage at Maximum Power (Vmp)	29.6 V
Current at Maximum Power (Imp)	7.94 A
Open circuit voltage (Voc)	36.7 V
Short circuit current (Isc)	8.48 A
Maximum Power temperature coefficient	−0.47%/°C
Open circuit voltage temperature coefficient	−0.32%/°C
Short circuit current temperature coefficient	+0.04%/°C
Operating temperature	−40~+85°C
Nominal operating cell temperature (NOCT)	45 ± 2°C
Number of cells (Nc)	60

Table 2: Adjusted parameters of the Altius AFP 235 at nominal operating conditions.

Name-Specifications from data sheet	AFP 235
Maximum Power (Pmax,m)	239.99 Wp
Voltage at Maximum Power (Vmpp)	29.6 V
Current at Maximum Power (Impp)	7.94 A
Open circuit voltage (Voc)	36.7 V
Short circuit current (Isc)	8.48 A
Nominal saturation current ($I_{0,n}$)	3.65412e − 010 A
Photovoltaic current (I_{pv})	8.490576 A
Diode ideality factor (a)	1.3
Series resistance (Rs)	0.318 Ω
Parallel resistance (Rp)	259.398 Ω

$$\begin{aligned} P_c &= \iiint \rho j^2 dV, \\ P_t &= \iiint \gamma c \frac{\partial \theta}{\partial t} dV, \\ P_r &= \iiint \operatorname{div}(\lambda \cdot \operatorname{grad} \theta)\, dV, \\ P_a &= \iiint k_t \frac{l}{S} (\theta - \theta_a)\, dV. \end{aligned} \tag{20}$$

Thus,

$$\begin{aligned} \iiint \rho j^2 dV = \iiint \gamma c \frac{\partial \theta}{\partial t} dV - \iiint \operatorname{div}(\lambda \cdot \operatorname{grad} \theta)\, dV \\ + \iiint k_t \frac{l}{S} (\theta - \theta_a)\, dV. \end{aligned} \tag{21}$$

The material density, specific heat, and thermal conductivity do not have an important temperature variation; thus they can be regarded as constants. On the other hand, the electrical resistivity has a significant temperature variation and can be estimated through a parabolic variation or a linear one. The experimental tests concluded that the difference between these two types of variation is not so important. For the electrical resistivity a linear variation with the temperature has been considered [32]:

$$\rho = \rho_0 [1 + \alpha (\theta - \theta_a)] \tag{22}$$

with the notation:

$$\vartheta = \theta - \theta_a. \tag{23}$$

Figure 17 shows the result of the thermal simulation for the ALTIUS Module AFP-235W for a nominal load of 235 W considered with a uniform distribution over the surface of the photovoltaic panel.

A temperature variation on the surface of the PV module is observed starting from a low temperature of 40.15°C to a high value of 52.07°C on the top of the surface of the PV module. This is explained because of variable thermal convection coefficient. This coefficient includes the circulation of the air flow from the lower side of the panel to the top. It was considered only natural to cool of the PV module and for the temperature of the environment to be 25°C.

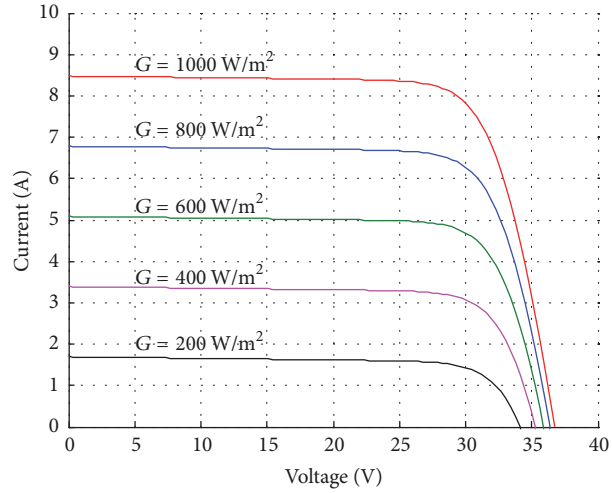

Figure 5: I-V curves for different solar irradiation.

6. Experimental Data for the PV Module

For the experimental analysis the photovoltaic panel ALTIUS Module AFP-235W was considered, oriented to the South and with an inclination of 45°. The experimental tests were realized on May 26, 2016 between 7.00 a.m. and 8 p.m. The solar irradiation was measured using a Solar Survey100/200R instrument, which is in compliance with the IEC-62446 international standard on PV systems. It measures the solar radiation to a maximum of 1500 W/m^2, with a resolution of 1 W/m^2. The temperature was measured with Extech 42545 IR thermometer (range: 50···1000°C, resolution: 0.1°C). A digital multimeter Fluke 115 was used to measure the voltage and current (resolution of 1 mV and 1 mA). Figure 18 shows the evolution of the temperature of the environment, the

Table 3: Properties of the materials used in AFP 235 module.

	Material	Thickness [mm]	Thermal conductivity, [W/mK]	Density [kg/m^3]	Specific heat [J/kgK]
1	Glass window	3.2	1.7	3000	780
2	EVA film	1	0.235	960	3135
3	PV cell	0.22	148	2330	710
4	White Polyester	1	0.25	1300	1350

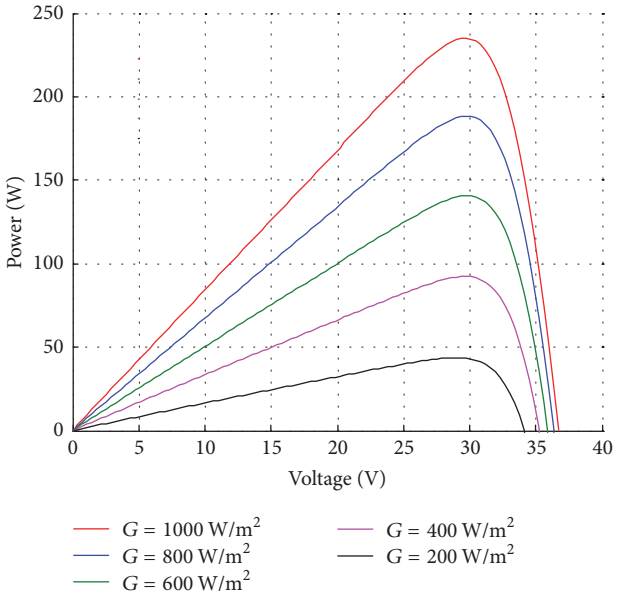

Figure 6: P-V curves for different solar irradiation.

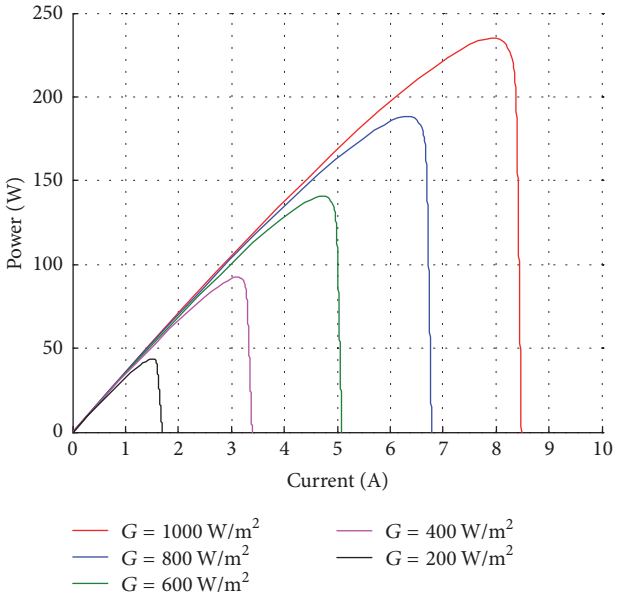

Figure 7: P-I curves for different solar irradiation.

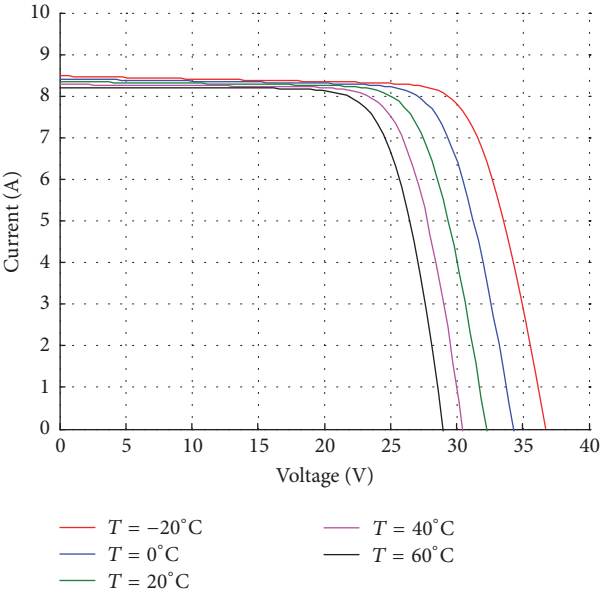

Figure 8: I-V curves for different cell temperatures.

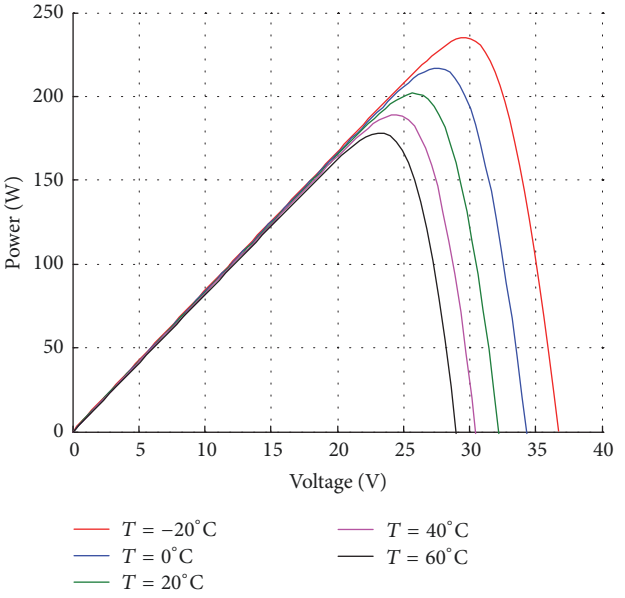

Figure 9: P-V curves for different cell temperatures.

temperature on the surface of the photovoltaic module, and the solar irradiation variation along the day. As the solar irradiation increases and is absorbed at the PV module surface, its temperature is increasing due to the photons absorption. At the maximum temperature of the environment of 28.3°C and a solar irradiation of 672 W/m^2, the temperature of the module surface reaches the value of 41.1°C.

In Figures 19, 20, and 21 the simulated and experimental I-V, P-V, and, respectively, P-I characteristics for the module PFV ALTIUS 235W for a medium temperature of 25°C and a

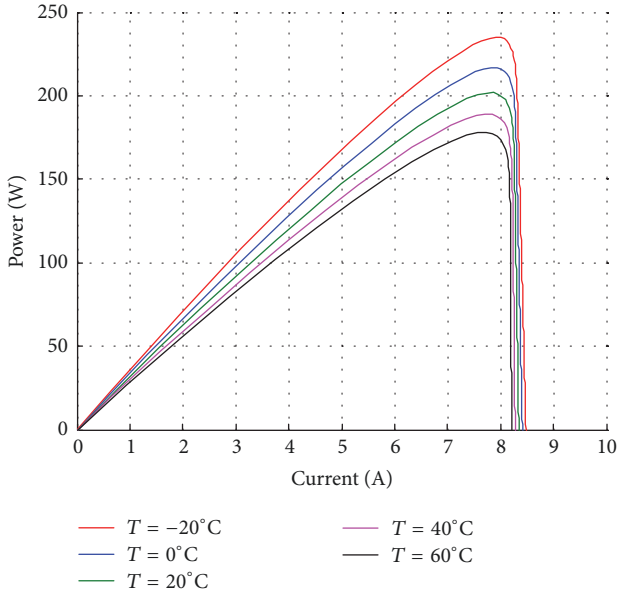

Figure 10: P-I curves for different cell temperatures.

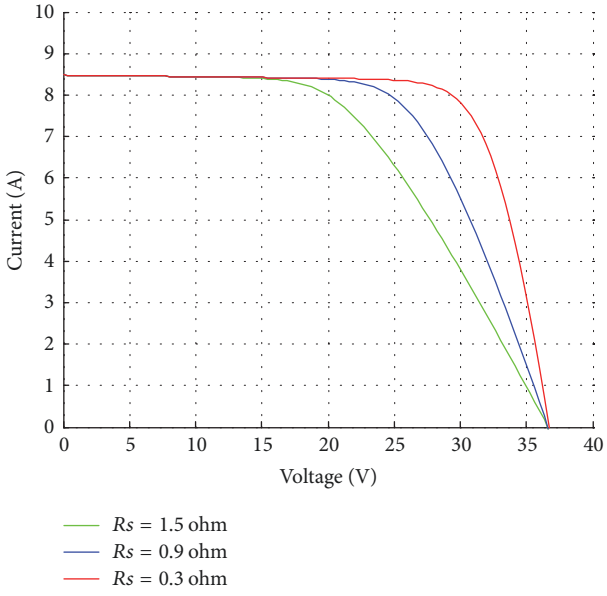

Figure 11: I-V curves for different R_s.

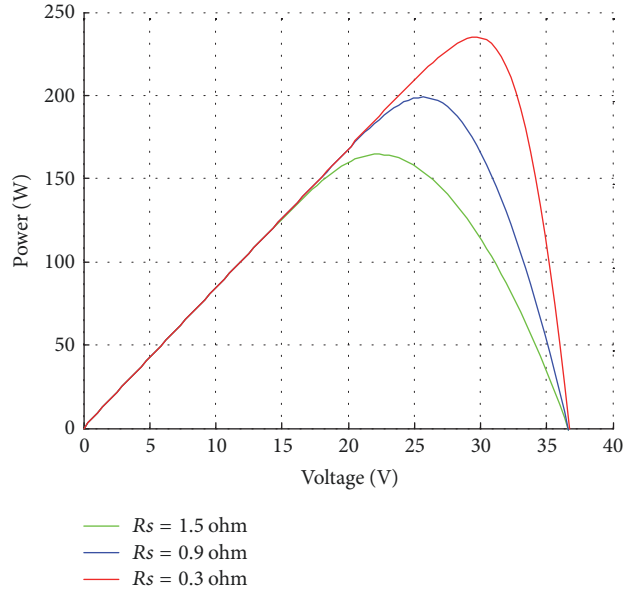

Figure 12: P-V curves for different R_s.

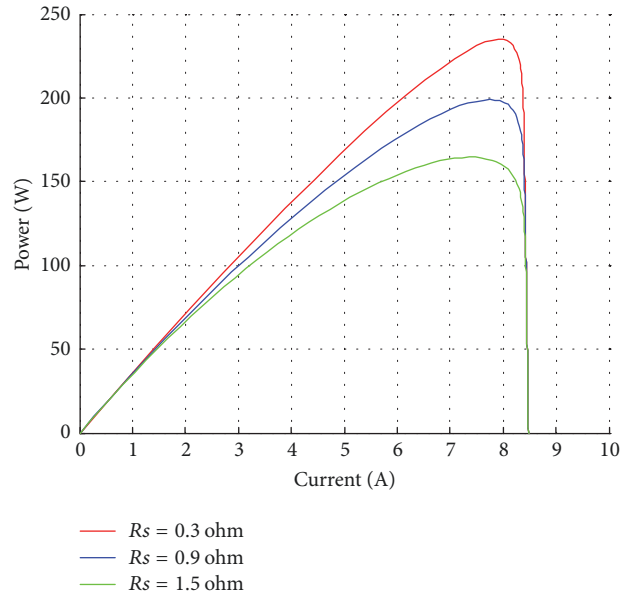

Figure 13: P-I curves for different R_s.

solar irradiation of 800 W/m^2 are plotted. The value of the nominal short circuit current is of $I_{sc,exp} = 8.35$ A for the experimental data and of $I_{sc,sim} = 8.48$ A for the simulation, with an error of 1.55%. The nominal open circuit voltage is of $V_{0c,exp} = 33.91$ V for the experimental characteristic and $V_{oc,sim} = 36.33$ V for the simulated one, with an error of −2,6%. In the Maximum Power Point the experimental values for the voltage and current are $V_{mpp,exp} = 27.79$ V, $I_{mpp,exp} = 6.628$ A, and a power of $P_{mpp,exp} = 184.92$ W, while the simulated resulted values are $V_{mpp,sim} = 25.55$ V, $I_{mpp,sim} = 7.55$ A, and a power of $P_{mpp,sim} = 192.9$ W. The error for the power estimation is about 4.3%. In these characteristics there are some differences between the simulated and the experimental data. For example on the point $(I_{sc,n})$, there is a difference of 0.13 A, on the point $(V_{0c,n})$, there is a difference of 2.42 V, and on the MPP point, there is a difference of 2.24 V and 0.982 A (7.98 W). These differences are due to the variation of the real temperature of the environment, of the solar irradiation, and consequently to the surface panel heating. Also the dust deposited on the panel surface and the wind has an important influence over the experimental data and thus on the difference between the simulated data and the experimental ones.

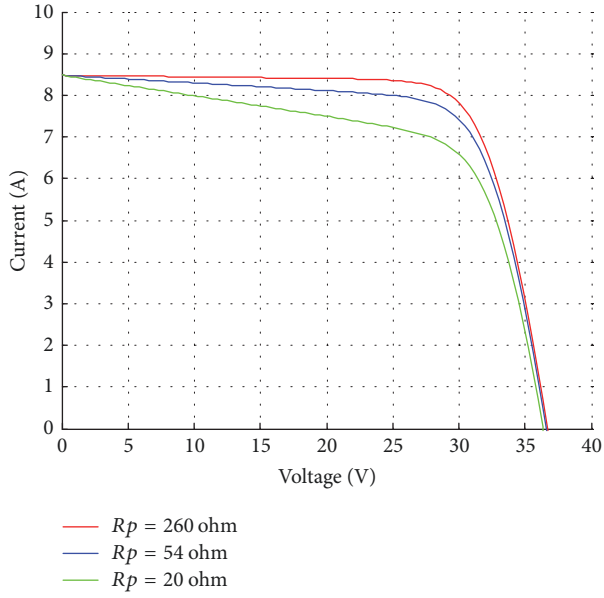

FIGURE 14: I-V curves for different R_p.

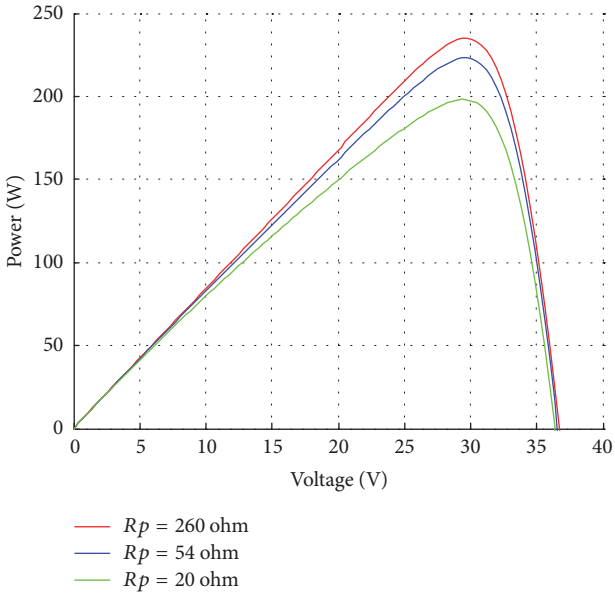

FIGURE 15: P-V curves for different R_p.

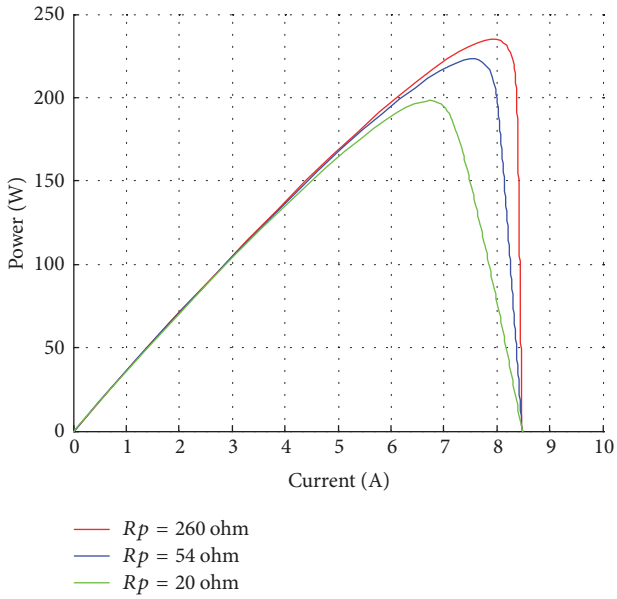

FIGURE 16: P-I curves for different R_p.

7. Conclusions

In this article a model of the photovoltaic module is developed and the influences of some parameters are analyzed as series and parallel resistances, temperature, and solar irradiation over the PV module output characteristics (I-V, P-V and P-I characteristics). For a real photovoltaic module (ALTIUS Module AFP-235W) there are estimated series and parallel resistances for which the energetical performances of the module have optimal values for a solar radiation of 1000 W/m^2 and a temperature of the environment of 25°C. Temperature influence over the PV module performances is analyzed by using a thermal model of the ALTIUS Module AFP-235W using the finite element method. A temperature variation on the surface of the PV module is estimated as a difference of about 12°C between the bottom and the top surface of the PV module. Experimental data are measured for the photovoltaic ALTIUS Module AFP-235W for an entire daylight. Differences between the simulated and recorded data are due to the variation of the real temperature of the environment, of the solar irradiation, and consequently to the surface panel heating. The dust deposited on the panel surface and the wind has an important influence over the

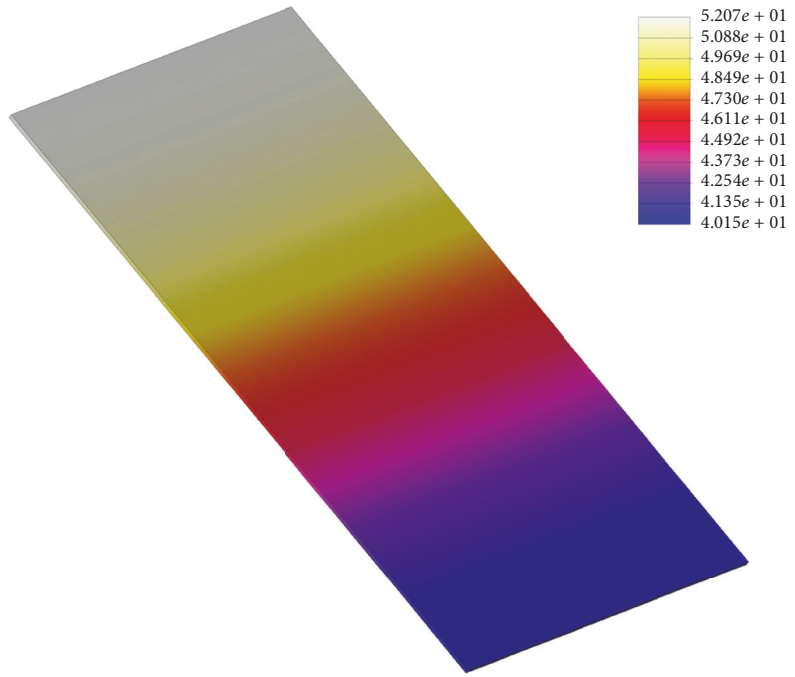

Figure 17: The temperature distribution for the PV module ALTIUS 235W.

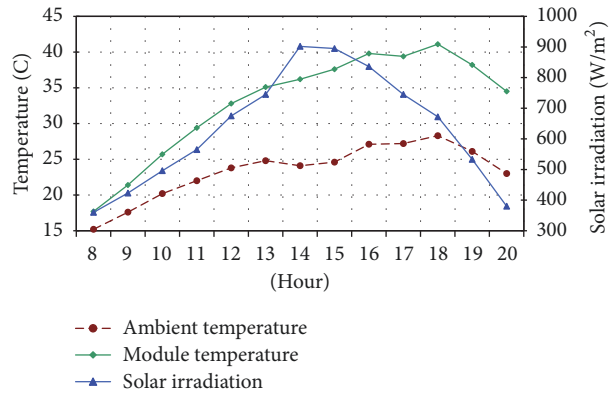

Figure 18: The T-t-G experimental characteristics for PFV ALTIUS 235W.

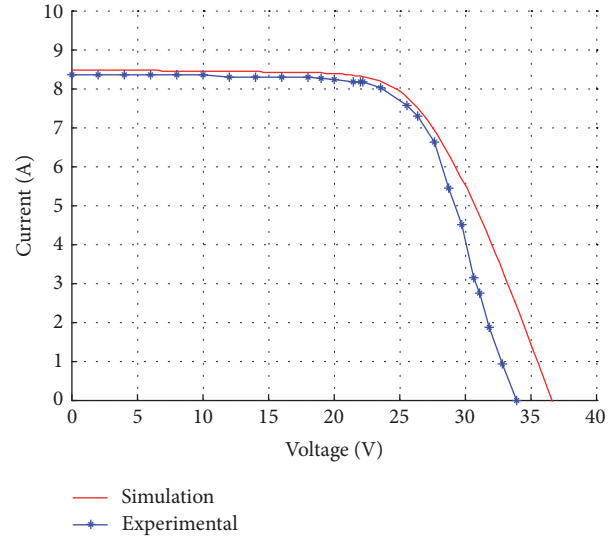

Figure 19: The I-V characteristics of PFV ALTIUS 235W.

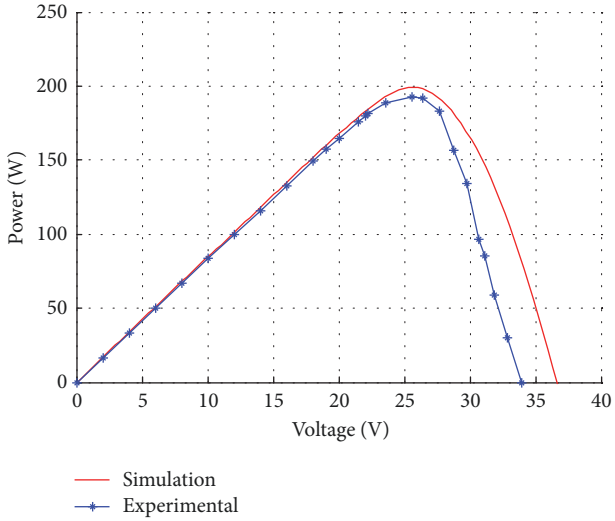

Figure 20: The P-V characteristics of PFV ALTIUS 235W.

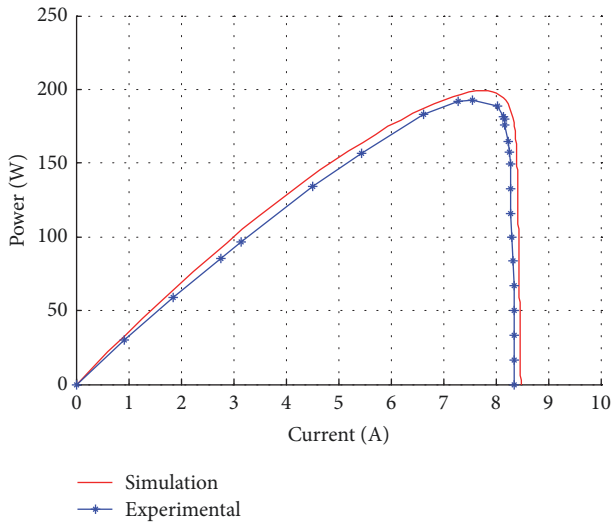

Figure 21: The P-I characteristics of PFV ALTIUS 235W.

experimental data and thus on the difference between the simulated data and the experimental ones.

Nomenclature

A_{cell}: The surface of the cell
a: The ideality factor of the diode, $1 \leq a \leq 1.5$
c: Specific heat
G: The incident irradiation
G_n: The nominal irradiation (usually 1000 W/m^2)
I_0: The reverse saturation current of the diode
$I_{0,n}$: The nominal saturation current
I_D: The diode current
I_{mpp}: The current at the MPP point
I_{pv}: The photovoltaic current of the PV cell
$I_{\text{pv},n}$: The photovoltaic current at nominal irradiation and temperature
$I_{\text{sc},n}$: The nominal short circuit current
j: Current density
K_V: The open circuit voltage temperature coefficient of the module
K_I: The short circuit current temperature coefficient of the module
k: The Boltzmann constant
k_t: Total transfer coefficient
l: Perimeter length of the external surface
MPP: Maximum Power Point
N_p: The number of the cells connected in parallel
N_s: The number of the cells connected in series
P_a: The thermal power dissipated to the environment area by the surface convection
P_c: The heating power from the current flow
$P_{\text{max},e}$: The maximum experimental power
$P_{\text{max},m}$: The maximum calculated peak output power
P_r: The power removed from the element by thermal conduction
P_t: The heat stored by temporal change of temperature
q: The electron charge
R_p: The equivalent parallel resistance of the module
R_s: The equivalent series resistance of the module
S: Surface convection
T: The ambient temperature
T_m: The nominal temperature (usually 25°C)
V: The open circuit voltage
$V_{0c,n}$: The nominal open circuit voltage of the module
V_T: The thermal voltage of the module
V_{mpp}: The voltage at the MPP
α: Coefficient of electrical resistivity variation with temperature
γ: Material density
λ: Thermal conductivity
ρ: Electrical resistivity
ρ_0: Electrical resistivity at the θ_a temperature
θ: Temperature
θ_0: The initial temperature of the photovoltaic module
θ_a: The temperature of the environment
$\vartheta = \theta - \theta_a$: As notation.

Conflicts of Interest

The authors declare that they have no conflicts of interest.

References

[1] R. Kumar and R. Muralidharan, "Mathematical modeling, simulation and validation of photovoltaic cells," *International Journal of Research in Engineering and Technology*, vol. 3, no. 10, pp. 170–174, 2014.

[2] T. Ahmad, S. Sobhan, and M. F. Nayan, "Comparative analysis between single diode and double diode model of PV cell: concentrate different parameters effect on its efficiency," *Journal of Power and Energy Engineering*, vol. 04, no. 03, pp. 31–46, 2016.

[3] H.-L. Tsai, C.-S. Tu, and Y.-J. Su, "Development of generalized photovoltaic model using MATLAB/Simulink," in *Proceedings of the World Congress on Engineering and Computer Science*, pp. 1–6, San Francisco, Calif, USA, 2008.

[4] B. Habbati, Y. Ramdani, and F. Moulay, "A detailed modeling of photovoltaic module using MATLAB," *NRIAG Journal of Astronomy and Geophysics*, vol. 3, pp. 53–61, 2014.

[5] M. G. Villalva, J. R. Gazoli, and E. R. Filho, "Modeling and circuit-based simulation of photovoltaic arrays," *Brazilian Journal of Power Electronics*, vol. 14, no. 1, pp. 35–45, 2009.

[6] Y. T. Tan, D. S. Kirschen, and N. Jenkins, "A model of PV generation suitable for stability analysis," *IEEE Transactions on Energy Conversion*, vol. 19, no. 4, pp. 748–755, 2004.

[7] A. Dev and B. Jeyaprabha, "Modeling and simulation of photovoltaic module in MATLAB," in *Proceedings of the International Conference on Applied Mathematics and Theoretical Computer Science*, pp. 268–273, 2013.

[8] A. M. Haque, S. Sharma, and D. Nagal, "Simulation of photovoltaic array using MATLAB/Simulink: analysis, comparison & results," *International Journal of Advanced Computer Technology*, vol. 3, no. 2, pp. 12–21, 2016.

[9] J. Park, H. Kim, Y. Cho, and C. Shin, "Simple modeling and simulation of photovoltaic panels using Matlab/Simulink," *Advanced Science and Technology Letters*, vol. 73, pp. 147–155, 2014.

[10] S. Sumathi, A. L. Kumar, and P. Surekha, *Solar PV and Wind Energy Conversion Systems. An Introduction to Theory, Modeling with MATLAB/Simulink, and the Role of Soft Computing Techniques*, Green Energy and Technology, Springer, New York, NY, USA, 2015.

[11] N. D. Benavides and P. L. Chapman, "Modeling the effect of voltage ripple on the power output of photovoltaic modules," *IEEE Transactions on Industrial Electronics*, vol. 55, no. 7, pp. 2638–2643, 2008.

[12] A. Kajihara and T. Harakawa, "Model of photovoltaic cell circuits under partial shading," in *Proceedings of the IEEE International Conference on Industrial Technology (ICIT '05)*, pp. 866–870, Hong Kong, China, December 2005.

[13] A. N. Celik and N. Acikgoz, "Modelling and experimental verification of the operating current of mono-crystalline photovoltaic modules using four- and five-parameter models," *Applied Energy*, vol. 84, no. 1, pp. 1–15, 2007.

[14] L. Cristaldi, M. Faifer, M. Rossi, and S. Toscani, "An improved model-based maximum power point tracker for photovoltaic panels," *IEEE Transactions on Instrumentation and Measurement*, vol. 63, no. 1, pp. 63–71, 2014.

[15] M. Veerachary, "PSIM circuit-oriented simulator model for the nonlinear photovoltaic sources," *IEEE Transactions on Aerospace and Electronic Systems*, vol. 42, no. 2, pp. 735–740, 2006.

[16] I. H. Altas and A. M. Sharaf, "A photovoltaic array simulation model for matlab-simulink GUI environment," in *Proceedings of the International Conference on Clean Electrical Power (ICCEP '07)*, pp. 341–345, Capri, Italy, May 2007.

[17] E. Matagne, R. Chenni, and R. El Bachtm, "A photovoltaic cell model based on nominal data only," in *Proceedings of the International Conference on Power Engineering, Energy and Electrical Drives (POWERENG '07)*, pp. 562–565, Setubal, Portugal, April 2007.

[18] Y. Lee and A. A. O. Tay, "Finite element thermal analysis of a solar photovoltaic module," *Energy Procedia*, vol. 15, pp. 413–420, 2012.

[19] W. Z. Leow, Y. M. Irwan, M. Irwanto, M. Isa, A. R. Amelia, and I. Safwati, "Temperature distribution of three-dimensional photovoltaic panel by using finite element simulation," *International Journal on Advanced Science, Engineering and Information Technology*, vol. 6, no. 5, pp. 607–612, 2016.

[20] N. Boulfaf and J. Chaoufi, "Identification of thermal parameters of a solar photovoltaic panel in three-dimensional using finite element approach," *International Journal of Renewable Energy Research*, vol. 7, no. 2, pp. 578–584, 2017.

[21] F. Montero-Chacón, S. Zaghi, R. Rossi et al., "Multiscale thermo-mechanical analysis of multi-layered coatings in solar thermal applications," *Finite Elements in Analysis and Design*, vol. 127, pp. 31–43, 2017.

[22] A. Massi Pavan, S. Vergura, A. Mellit, and V. Lughi, "Explicit empirical model for photovoltaic devices. Experimental validation," *Solar Energy*, vol. 155, pp. 647–653, 2017.

[23] F. Sarhaddi, S. Farahat, H. Ajam, A. Behzadmehr, and M. Mahdavi Adeli, "An improved thermal and electrical model for a solar photovoltaic thermal (PV/T) air collector," *Applied Energy*, vol. 87, no. 7, pp. 2328–2339, 2010.

[24] J. Yazdanpanahi, F. Sarhaddi, and M. Mahdavi Adeli, "Experimental investigation of exergy efficiency of a solar photovoltaic thermal (PVT) water collector based on exergy losses," *Solar Energy*, vol. 118, pp. 197–208, 2015.

[25] Altius module high performance solar modules, AFP 60-250 Series/235-250W.

[26] D. Sera, R. Teodorescu, and P. Rodriguez, "PV panel model based on datasheet values," in *Proceedings of the IEEE International Symposium on Industrial Electronics (ISIE '07)*, pp. 2392–2396, Vigo, Spain, June 2007.

[27] A. Driesse, S. Harrison, and P. Jain, "Evaluating the effectiveness of maximum power point tracking methods in photovoltaic power systems using array performance models," in *Proceedings of the PESC 07 - IEEE 38th Annual Power Electronics Specialists Conference*, pp. 145–151, Orlando, Fla, USA, June 2007.

[28] R. A. Messenger and J. Ventre, *Photovoltaic Systems Engineering*, CRC Press, Boca Raton, Fla, USA, 2004.

[29] J. Crispim, M. Carreira, and C. Rui, "Validation of photovoltaic electrical models against manufacturers data and experimental results," in *Proceedings of the International Conference on Power Engineering, Energy and Electrical Drives, POWERENG 2007*, pp. 556–561, Setubal, Portugal, April 2007.

[30] N. M. Abd Alrahim Shannan, N. Z. Yahaya, and B. Singh, "Single-diode model and two-diode model of PV modules: a comparison," in *Proceedings of the 2013 IEEE International Conference on Control System, Computing and Engineering, ICCSCE 2013*, pp. 210–214, Mindeb, Malaysia, December 2013.

[31] V. Sangsawang and S. Chaitusaney, "Modeling of photovoltaic module from commercial specification in datasheet," in *Proceedings of the 9th International Conference on Electrical Engineering/Electronics, Computer, Telecommunications and Information Technology, ECTI-CON 2012*, Phetchaburi, Thailand, May 2012.

[32] A. T. Plesca, "Thermal analysis of the current path from circuit breakers using finite element method," *International Journal of Electrical, Computer, Energetic, Electronic and Communication Engineering*, vol. 6, no. 12, pp. 1479–1487, 2012.